II. RADIO ASTRONOMY

Academic and Research Staff

Prof. A. H. Barrett
Prof. B. F. Burke
Prof. Susan G. Kleinmann
Prof. R. M. Price

Prof. D. H. Staelin
Dr. P. L. Kebabian
Dr. K. F. Kunzi
Dr. P. C. Myers
Dr. G. D. Papadopoulos

Dr. J. Sander
Dr. J. W. Waters
J. W. Barrett
D. C. Papa

Graduate Students

B. G. Anderson
O. Appiah
K. P. Bechis
W. G. Brodsky
P. C. Crane
R. W. Freund

T. S. Giuffrida
A. D. Haschick
P. T. Ho
K-S. Lam
S. Lee
K-Y. Lo
R. N. Martin

R. V. McGahan
R. L. Pettyjohn
R. K. L. Poon
R. C. Walker
T. J. Warren
R. W. Wilcox

A. ANOMALOUS OXYGEN ABSORPTION INFERRED FROM NIMBUS-5 MICROWAVE EXPERIMENT

R. K. L. Poon, D. H. Staelin

Atmospheric absorption near 5-mm wavelength is dominated by oxygen. We shall describe 10 methods for computing its absorption coefficient (see Expressions 1-10 in Table II-1). The pressure-broadening theories of Van Vleck and Weisskopf (VV-W)[1] and of Gross and Reber (G-R)[2] lead to different spectral line shapes (Methods 1 and 2). One major uncertainty associated with these theories is the linewidth, whose value has been experimentally determined but not well explained.[3] For this reason, we have developed Expressions 3-10 in Table II-1.

We assume that the absorption coefficient k varies with total air pressure p as $k = a p^x$, where a and x are frequency-dependent parameters. Good fit of this expression to Methods 1 and 2 is obtained when a and x are determined by regressing k against pressure from 10 to 1000 mb. The regression is performed on a sample of pressure-temperature pairs that occur in the ARDC model.[4] This yields Expressions 3 and 4, respectively, for the two line shapes. As a check, a "random sample" is prepared with pressures and temperatures T independently chosen in the range of atmospheric interest. Regression is then performed on this "random sample" in the form $k = a p^x$ (Expressions 5 and 6) and in the form $k = a p^x T^y$ (Expressions 7 and 8).

Table II-1 shows the result of different expressions of regression in the general normalized form $k = k_0 (p/p_0)^x (T/T_0)^y$. The parameters k_0, x, and y give best fit to Method 1 values when we use Expressions 3, 5, or 7 for regression. Expressions 2, 4, 6, and 8 are counterparts referred to the Gross-Reber (G-R) line shape. The parameters

Table II-1. Parameters inferred from different expressions of regression in the normalized form $k = k_o(p/p_o)^x (T/T_o)^y$.

| PARAMETER		CH	1	3	5	7	2	4	6	8	9	10
k_o	p_o = 617 mb	3	0.191	0.189	0.192	0.192	0.181	0.178	0.182	0.182	0.186	0.244
	p_o = 265 mb	4	0.203	0.195	0.199	0.198	0.174	0.167	0.170	0.170	0.232	0.247
	p_o = 89 mb	5	0.302	0.297	0.293	0.293	0.239	0.241	0.242	0.242	0.339	0.772
x		3	—	1.26	1.29	1.29	—	1.28	1.25	1.24	1.3	1.5
		4	—	1.40	1.32	1.32	—	1.47	1.45	1.45	1.54	1.75
		5	—	1.79	1.57	1.57	—	1.51	1.48	1.48	2.05	4
y	T_o = 262°K	3	—	0	0	−0.10	—	0	0	−0.07	0	0
	T_o = 223°K	4	—	0	0	−0.21	—	0	0	−0.15	0	0
	T_o = 217°K	5	—	0	0	−0.96	—	0	0	−0.84	0	0
NEMS Channel Frequencies 3 53.65 GHz 4 54.9 GHz 5 58.8 GHz			Exact	ARDC (p, T)	Random (p, T)		Exact	ARDC (p, T)	Random (p, T)		Nimbus-5 User's Guide WF	NEMS Data
				VV-W Line Shape				G-R Line Shape				
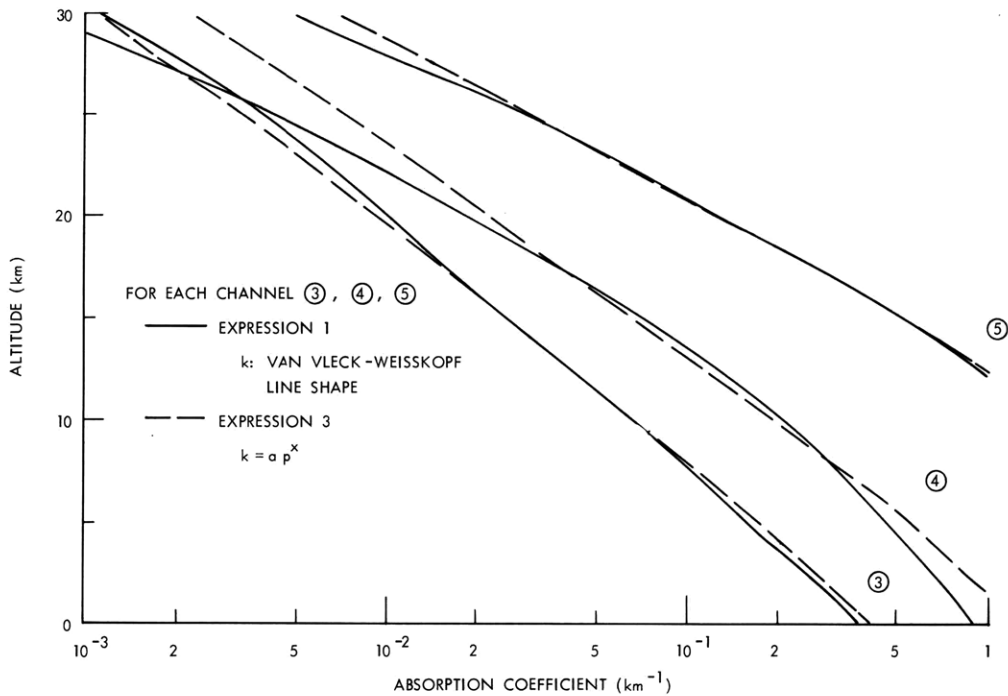
Fig. II-1. Fitted absorption coefficient for the ARDC model atmosphere.

are given for the absorption at 53.65, 54.9, and 58.8 GHz, three center frequencies near the 5-mm oxygen resonances (Channels 3, 4, 5) which have been selected for the Nimbus-5 Microwave Experiment (NEMS).[5] Figure II-1 shows the good fit of Expression 3 to the ARDC model atmosphere.

The form $k = a p^x$ leads to a surprisingly simple description of the temperature weighting function (WF), defined[3] as $k(z) \exp[-\tau(z)]$, which takes on the simple form $s \exp -[sz^* + \exp(-sz^*)]$ at any height z, where $s = x/H$, $z^* = z - z_m$ is the height referenced at the WF peak height $z_m = \frac{1}{s} \ln \frac{a\, p_o^x}{s}$, and the atmospheric pressure p is assumed to equal p_o at the surface of the Earth and decrease exponentially with a scale height H. The opacity at z is $\tau(z) = \int_z^\infty k(z)\, dz = k(z)/s$. In particular, at the WF peak, $\tau(z_m) = 1$, while $k(z_m) = s$, or roughly 1 dB/km, since $x \sim 1.5$, $H \sim 7$ km and 1 neper ~ 4.343 dB. The peak value of the WF is s/e, which reduces to a fraction f of the peak value when the shoulder width of the WF is c/s, where c is a tabulated function of f (for example, c = 2.45 at f = 0.5). The exact relationships derived from the form $k = a p^x$ are shown in Fig. II-2. They help us to fit a given WF by a judicious choice of a and x (Method 9). In Table II-1 the normalization constants p_o and T_o are the pressures and temperatures where the three weighting functions peak. Figure II-3 shows the result of fitting the NEMS weighting function as given in "The Nimbus-5 User's Guide."[5]

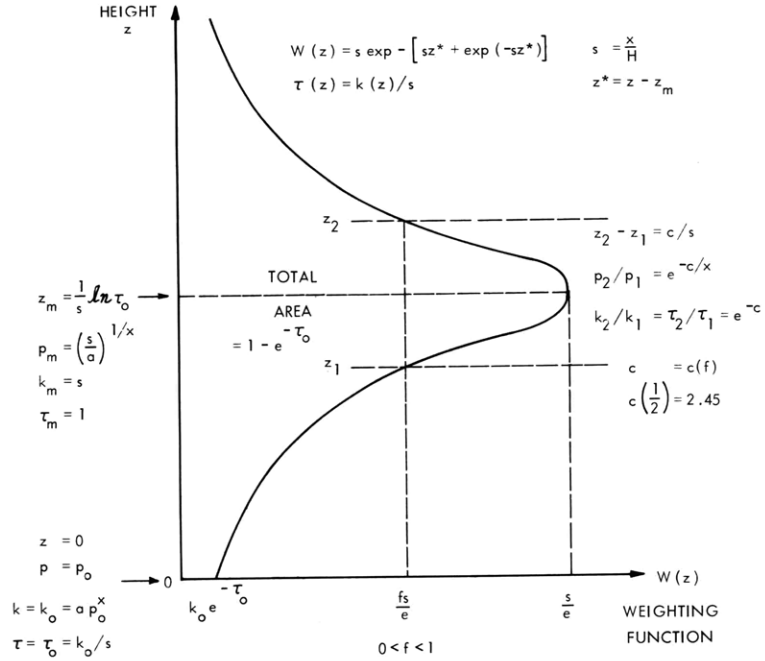This form of WF, in conjunction with the radiative transfer equation, is used to

$$W(z) = s \exp - \left[sz^* + \exp(-sz^*) \right] \qquad s = \frac{x}{H}$$

$$\tau(z) = k(z)/s \qquad z^* = z - z_m$$

z_2

$z_2 - z_1 = c/s$

$z_m = \frac{1}{s} \ln \tau_o$

TOTAL

AREA

$= 1 - e^{-\tau_o}$

$P_2/P_1 = e^{-c/x}$

$k_2/k_1 = \tau_2/\tau_1 = e^{-c}$

$p_m = \left(\frac{s}{a} \right)^{1/x}$

$k_m = s$

$\tau_m = 1$

z_1

$c = c(f)$

$c\left(\frac{1}{2} \right) = 2.45$

$z = 0$

$p = p_o$

$k = k_o = a \, p_o^x$

$\tau = \tau_o = k_o/s$

$k_o e^{-\tau_o}$

$\frac{fs}{e}$

$\frac{s}{e}$

$W(z)$

WEIGHTING

FUNCTION

$0 < f < 1$

Fig. II-2. Exact relationships of the analytic weighting function.

$$W = k \, e^{-\frac{H}{x} k}, \qquad k = a \, p^x$$

$$p = 1000 \, e^{-z/7 \text{ km}}$$

— — — WEIGHTING FUNCTIONS IN THE NIMBUS 5 USER'S GUIDE

⑤ 58.88 GHz
$x = 2.05$
$a = 3.49 \times 10^{-5}$

④ 54.94 GHz
$x = 1.54$
$a = 5.03 \times 10^{-5}$

③ 53.65 GHz
$x = 1.3$
$a = 4.91 \times 10^{-5}$
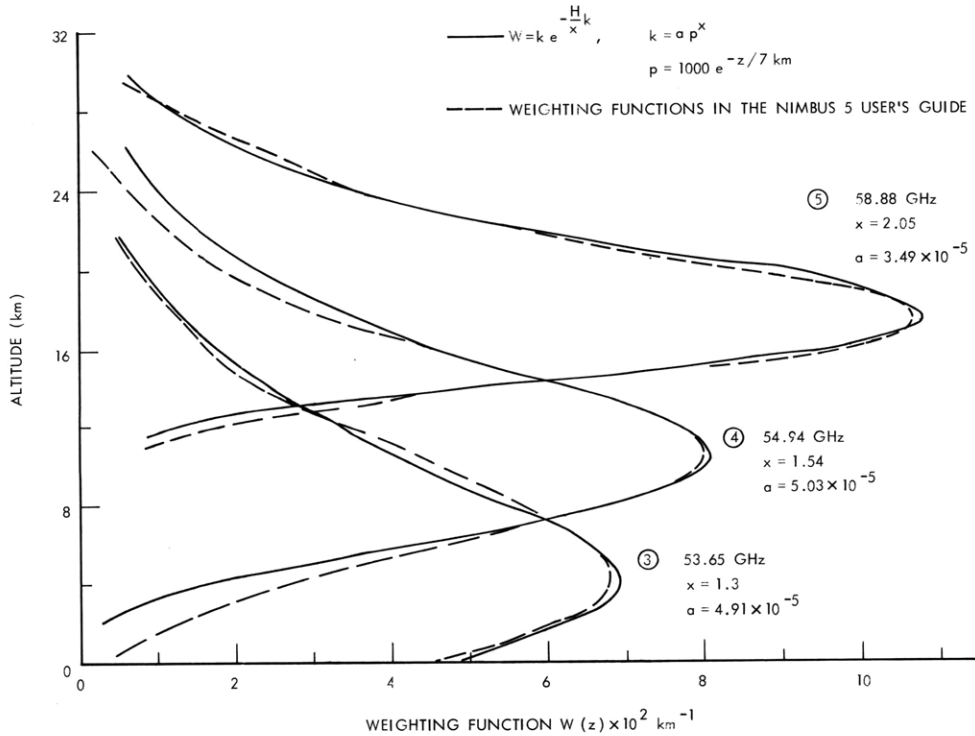
WEIGHTING FUNCTION $W(z) \times 10^2$ km^{-1}

Fig. II-3. Fitted weighting functions for the NEMS oxygen channels.

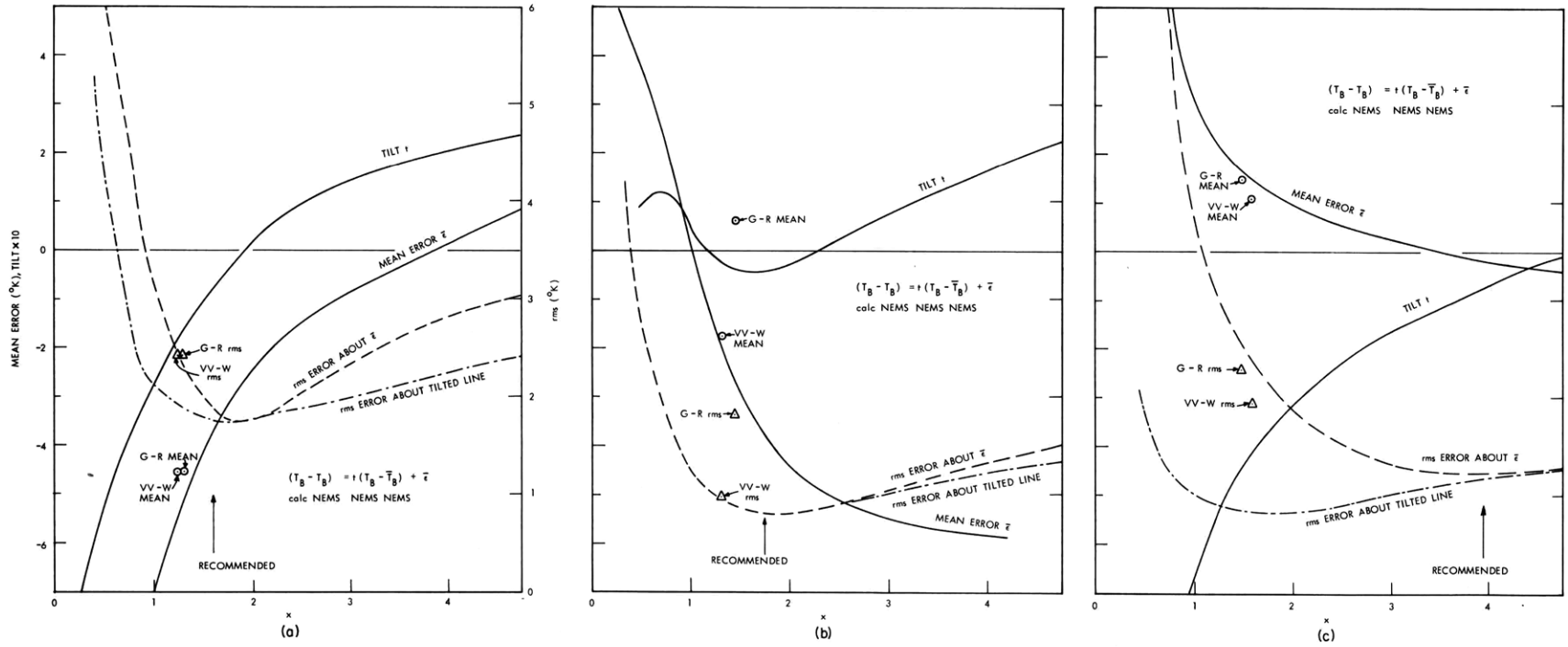Fig. II-4. Brightness-temperature error: (a) Channel 3, (b) Channel 4, (c) Channel 5.

calculate brightness temperatures $T_{B,calc}$ for comparison with NEMS measured values $T_{B,NEMS}$ for 100 major frames of data (December 1972) with wide spatial and temporal extent (Method 10). At each NEMS frequency, a and x are varied as free parameters in computing the absorption for the subsatellite temperature profile as analyzed by the National Oceanic and Atmospheric Administration (NOAA). We base our comparison on 4 error criteria: (i) mean error $\bar{\epsilon}$, which is the average of the discrepancy $\epsilon = T_{B,calc} - T_{B,NEMS}$; (ii) tilt t, defined as $\epsilon = t(T_{B,NEMS} - \bar{T}_{B,NEMS}) + \bar{\epsilon}$; (iii) rms error about $\bar{\epsilon}$; and (iv) rms error about the tilted line. (In these expressions, overbars denote averaging over the 100 major frames.) These discrepancies depend much more on x than on a. In Fig. II-4 the x dependence is shown for the value of a that gives the least rms about $\bar{\epsilon}$. Besides uncertainty in the absorption coefficient, there is inherent discrepancy associated with instrumental noise, error in the NOAA analysis, and other approximations in the radiative transfer computation. Everything considered, however, we recommend the values x = 1.5, 1.75, and 4 for Channels 3, 4, and 5, respectively, and z_m = 4, 9.25, and 17.5 km. This suggests more absorption than is given by the VV-W line shape, which in turn predicts more absorption than is given by the G-R line shape, at least near the peak of each WF. Absorption measurements with a Fabry-Perot interferometer are being made in our laboratory to resolve the present discrepancy.

References

1. J. H. Van Vleck, "The Absorption of Microwaves by Oxygen," Phys. Rev. 71, 413-424 (1947); J. H. Van Vleck and V. F. Weisskopf, "On the Shape of Collision Broadened Lines," Rev. Mod. Phys. 17, 227 (1945).

2. E. E. Reber, "Absorption of the 4- to 6-mm Wavelength Band in the Atmosphere," J. Geophys. Res. 77, 3831-3845 (1972).

3. M. L. Meeks and A. E. Lilley, "The Microwave Spectrum of Oxygen in the Earth's Atmosphere," J. Geophys. Res. 68, 1683-1703 (1963).

4. R. A. Minzner, K. S. W. Champion, and H. L. Pond, "The ARDC Model Atmosphere, 1959," AFCRC-TR-59-267, Air Force Surveys in Geophysics No. 115, Geophysics Research Directorate, Air Force Cambridge Research Center, U. S. Air Force, Bedford, Massachusetts, August 1959.

5. R. R. Sabatini (Ed.), "The Nimbus-5 User's Guide," Goddard Space Flight Center, National Aeronautics and Space Administration, Greenbelt, Maryland, November 1972.

B. STELLAR INTERFEROMETER: DIGITAL FILTERS

P. L. Kebabian

In previous studies of digital filters with variable sampling rate[1,2] the input to the filter was a time series of numbers. Obviously, all results derived for that case also apply to the case of parallel processing of numbers stored in a table. When the impulse response of the filter is of finite duration, which is almost always true of filters of practical interest (cf. Schafer and Rabiner[3]), it is possible to build such a parallel processor to obtain any given sample of the filter's output. This is no advantage in the case of rate-reducing filters, but it provides an attractive way of using a rate-increasing filter to interpolate between numbers stored in a table, in particular in a table of cosines.

Consider the rate-increasing filter in Fig. II-5a. The input sequence is $w_0, w_1, w_2,$ ..., and the output of the rate-increasing sampler is $w_0, 0, 0, \ldots, w_1, 0, 0, \ldots,$ with $r-1$ zeros added after each input number. The time-invariant filter interpolates between these numbers to produce the output sequence $y_0, y_1, y_2, \ldots$. Figure II-5b shows the equivalent parallel processor to generate y_1. Note that the filter h_j must be causal ($h_{j<0} = 0$), but there is no similar restriction on the coefficients in the parallel processor.

Figure II-6 shows the spectrum at the input to the filter, after the sampler, and at the output when the w are samples of a cosine function, $w_j = A \cos(2\pi j/N)$. $H(f)$ is the frequency response of the filter h_j and, by assumption, $\sum_j h_j = 1 = H(0)$. Ideally, the only components of the output would be at 1 and $(r-1)N$, and the design of the filter is governed by the tolerance on the components at $N\pm 1$, $2N\pm 1$, etc. For a given tolerance, as r increases the number of coefficients also increases, but because only $1/r$ of the samples
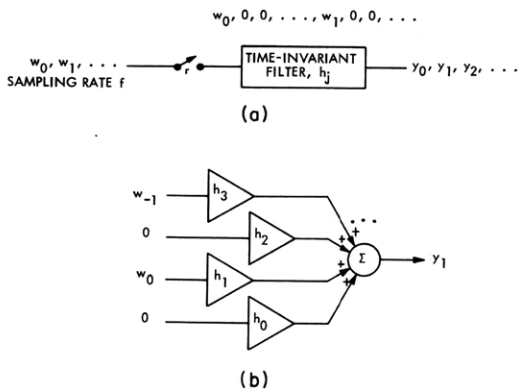

Fig. II-5. (a) Interpolation in a time series.
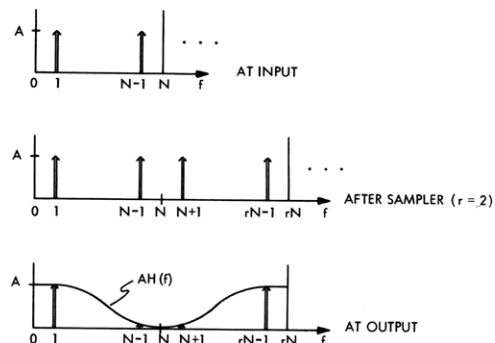(b) Parallel interpolation, for the case r = 2.

Fig. II-6. Signal spectra.

sent to the filter are nonzero the number of multiplications per second (in Fig. II-5a) stays the same. For very large r, the memory required for the coefficients becomes impractically large, and this prevents realizing the interpolator as a single unit cell such as in Fig. II-5.

As shown elsewhere,[2] both rate-decreasing and rate-increasing filters are realizable as a cascade of unit cells, the total rate change being the product of the rate changes of the separate cells. Realizable, in this case, means only that the filter in each cell is causal, and that the coefficients in the impulse response may be calculated from the cell's rate change, the overall rate change, and the overall impulse response. In general, the duration of the cell impulse responses is infinite, even when the overall impulse response has a finite duration. There is, however, one family of functions, $f(b)$, that generate sets of duplicating filters all of which have finite duration.[2] These are $f_n(b) = 1 + [b/n]$, $n \geq 1$, $b \geq 0$, together with $f_0(b) = 1$ (for $b<0$, $f(b) = 0$ in both cases), also with convolutions of these with each other. For example, f_0 generates the

duplicating filters that comprise a single boxcar integrator. Likewise, $f_0 * f_0$ (which is also f_1) generates the duplicating filters that comprise two boxcar integrators in cascade. An important remaining theoretical question is, Under what circumstances will the duplicating filters used to realize a given finite-duration impulse response filter with rate change all have finite-duration impulse responses?
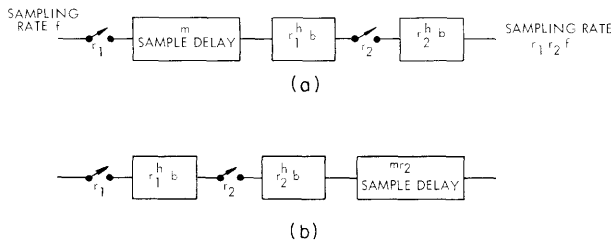

Fig. II-7.   (a) Chain with a delay.
             (b) Equivalent chain.

One of the elementary properties of a cascade of unit cells (Fig. II-7a) is that a time delay associated with the filter may be moved to the high sampling rate end of the chain, as in Fig. II-7b.

Assume that the chain has n stages, each having a rate increase of 2, and a filter with a symmetrical, finite-duration impulse response with 0 time delay. Now let a time delay of $d < 2^n$ samples be inserted after the output of the chain; $d/2^n = d_1 2^{-1} + d_2 2^{-2} + \ldots + d_n 2^{-n}$, $d_j = 0$ or 1. This is equivalent to a chain having d_1 samples delay in series with the first filter, d_2 in series with the second filter, and so forth. Suppose that the input is a sequence of samples from a cosine function, as before, with $N = 2^m$, and that A and the filter impulse responses are such that the output is a suitably accurate sequence of samples, at 2^n higher sampling rate, from a cosine function. By selecting

the initial phase of the input sequence and d_1 through d_n, the output at index 0 is the cosine of any angle, represented as an n+m bit binary fraction of a circle.   Since the filter impulse responses have finite duration, only a finite number of input samples is needed, usually «N.

This is the central idea of the present interpolation method: a 2^m word read-only-memory (ROM) and n unit cells simulates a 2^{n+m} word ROM, which might be far too large to be built directly.

Assume that each of the filters in the unit cells has an odd number of points, k+1, in its impulse response. As noted by Schafer and Rabiner,[3] this should be true of the filter to which the chain is equivalent because otherwise there will be a 1/2 sample phase shift; that is, the interpolator would not generate cos (0).   Let the input to the chain transmit k+1 samples to the rate-increasing sampler, which interleaves k+1 zeros and thus transmits 2k+2 samples to the filter, the indices of the samples being from −k through (k+1).   When the coefficient d of the unit cell is zero, the filter uses samples with indices −k/2 through k/2 in computing the output sample with index 0; −k through 0 for the output of index −k/2; and 0 through k for the output of index k/2.   If d = 1, the highest index input sample used is k+1.   Thus, the k+1 input samples are all that are needed to find k+1 output samples, and therefore the parallel processor may have any number of identical unit cells.   Figure II-8 shows an example for k = 2.
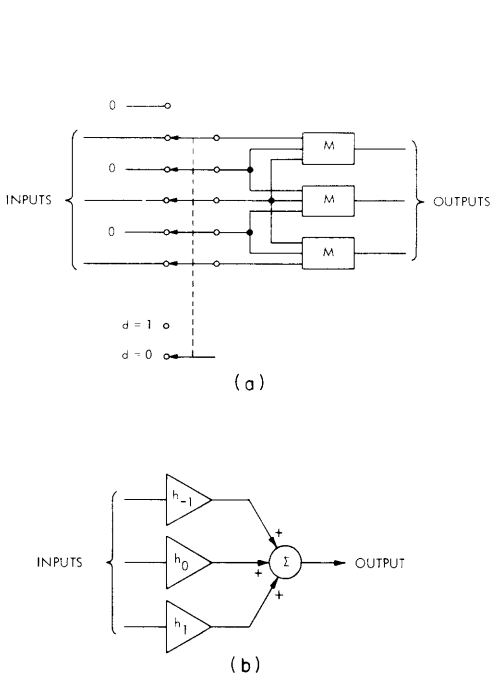

Fig. II-8.   (a) Parallel unit cell.
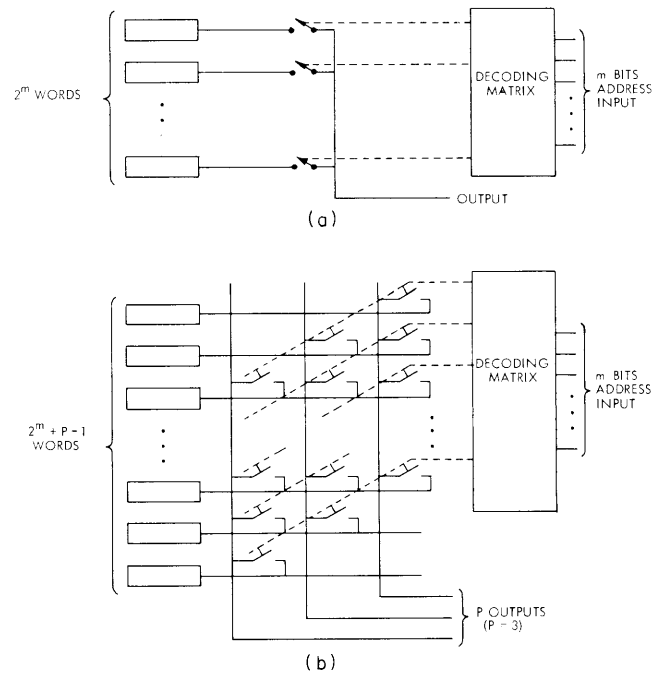   (b) Network M.

Fig. II-9.   (a) Conventional read-only-memory (ROM).
              (b) Modified ROM.

The ROM may store samples from the entire cosine function, or from just one quadrant. In that case, means must be provided to convert the address to that quadrant, and to multiply the outputs by ± 1 as needed. Because the input to the interpolator uses several consecutive entries from this memory, it differs from the conventional ROM, as illustrated in Fig. II-9.

Duplicating filters, as used for time-series filtering, are inherently discrete-time filters, but not necessarily digital, except to the extent that analog delay elements such as charge-coupled devices are not generally available. This limitation does not apply to the parallel processors described above in which it is perfectly possible for all the signals to be analog. In that case, this system is a form of digital-to-analog converter, in which the output is the cosine of the input number. The practical constraints determining the best structure of the unit cell are very different from those that apply to the case of digital signals, and it remains to be seen if this kind of D/A converter would be competetive with more conventional methods.

In the digital case, errors in the output result from errors in the numbers in the ROM, rounding errors in the unit cell, and errors inherent in the quantized angle, all in addition to the unwanted frequencies transmitted by the filter. Thus, all parts of the system must use a word length comparable to that of the output, and this, as well as the fact that each unit cell has several parallel data paths, means that bit-parallel representation of the numbers would involve an excessive amount of circuitry. Using bit-serial numbers simplifies the structure of the ROM, since a simple shift register will drive the bit-select lines, instead of a complete decoder.

The filters in the unit cells contain a cascade of k boxcar integrators. This structure, as shown in Fig. II-10 for the case k = 4, has the advantage of being built from a regular array of serial adders, and thus is suitable for large-scale integration. For this kind of filter, the only significant unwanted components in the spectrum are at
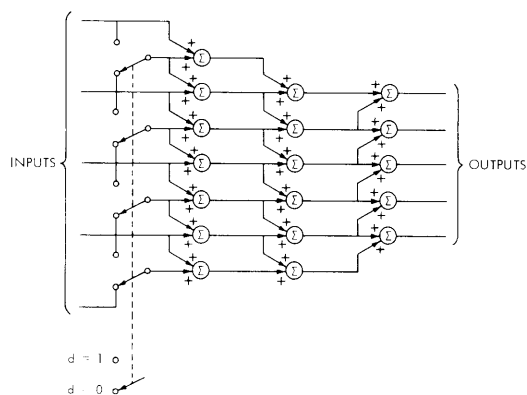

Fig. II-10.   Unit cell built from 4 cascaded boxcar integrators.

$N \pm 1$, with images at $(r-1)N \pm 1$. These have amplitude $\approx (1/N)^k$, $= 2^{-mk}$ for $N = 2^m$. They must produce negligible error compared with the quantization error, and thus $2^{-mk+1+t} < 2^{-(m+n)}$, or $k(m) \geqslant (m+n+t+1)/m$, where t is the tolerance in bits (typically 2). Also, k must be even so that the number of points in the impulse response is odd.

Each word in the ROM has length m+n+k+t' bits, where m+n is the length of the output, k is the increase in length within one unit cell before the number is rounded to form the cell's output, and t' is the tolerance to insure that the rounding error in the filter is negligible compared with the quantization error (typically 2 bits). Assume the ROM can have, at most, a total of 2^S bits, and that only one quadrant of the function is stored; s = 13 is reasonable, given the current state of the art, and the greater complexity of this kind of ROM. Then $2^m(m+n+k+t') < 2^S$ is a limit that must be satisfied by k(m), and m should be as large as possible, since for fixed n+m the computation time is proportional to n.

Each unit cell rounds the outputs from the adder array, and resynchronizes them by adding a delay of at least one bit. It is possible to use a real chain of separate unit cells, but a better way to get the same result is to store the outputs in shift registers, and at the end of each interpolation return them to the input of the same unit cell for the next interpolation. While this is happening, the ROM may send a new set of numbers to another unit cell, thereby effectively doubling the computation speed in the ordinary case when both the sine and cosine of an angle are used.

Table II-2 summarizes the performance of the system. The times are in units of the clock period of the serial data. If this is conservatively taken to be 1 μs, the times compare favorably with the 1-2 ms required for a typical 16-bit general-purpose computer (NOVA 1200) with hardware multiply/divide to compute a 24-bit answer.

Table II-2.   System performance.

m+n Bits	m	k	Number of Adders $=k^2+k/2$	Time
16	8	4	18	176
24	8	4	18	480
32	7	6	39	1000
64	6	12	150	4500

The advantage of this kind of cosine generator is that it requires relatively little circuitry and is comparable in speed to a small general-purpose computer with hardware multiply/divide. In computers without such a multiplier, it will greatly increase

the speed of jobs such as spectral analysis, and in computers with one it will increase
the speed somewhat, by permitting a measure of parallelism in operation of the program.

References

1. P. L. Kebabian, Quarterly Progress Report No. 101, Research Laboratory of Elec-
    tronics, M. I. T., April 15, 1971, pp. 1-11.

2. P. L. Kebabian, Ph. D. Thesis, Department of Electrical Engineering, M. I. T.,
    1972.

3. R. Schafer and L. Rabiner, Proc. IEEE 61, 692 (1973).